J. Physiol. (1973), **230**, *pp.* 29–50
With 3 plates and 5 text-figures
Printed in Great Britain

THE NEURAL SIGNAL OF ANGULAR HEAD POSITION IN PRIMARY AFFERENT VESTIBULAR NERVE AXONS

BY P. R. LOE,* DAVID L. TOMKO† AND G. WERNER

From the Department of Pharmacology, School of Medicine, University of Pittsburgh, Pittsburgh, Pennsylvania 15213, U.S.A.

(*Received 5 July 1972*)

SUMMARY

1. The relation between discharge frequency and angular head position was determined for a population of regularly discharging single first-order vestibular neurones in the eighth nerve of the barbiturate anaesthetized cat.

2. Each axon had a characteristic head position which was maximally excitatory to it, and a diametrically opposed head position which was minimally excitatory.

3. After correction for phase shifts introduced by the orientation of preferred excitability, discharge rate in statoreceptor afferents varied as a power function of the sine of angular head position with exponents ranging from 0·9 to 1·6.

4. Experimentally determined discharge rates were compared with the predictions of a computer simulation model incorporating the idea that shearing force acting on morphologically polarized receptors is the adequate stimulus for macular receptor cells.

5. This approach permitted the identification of a population of first-order vestibular afferents whose discharge frequency varied with head position as did the magnitude of shear force computed for individual receptors, each most excited in a particular head position.

6. The majority of the spatial orientations of maximal sensitivity defined a surface which is tilted by approximately 30° with reference to the Horsley–Clarke horizontal plane, implying that most statoreceptor afferents are maximally sensitive to position changes when the cat's head is at or near its normal position.

* Present address: Department of Physiology, University of North Carolina School of Medicine, Chapel Hill, N.C. 27514, U.S.A.

† Please address reprint requests to Dr David L. Tomko.

INTRODUCTION

The detailed anatomical investigations of Retzius (1881) provided the morphological evidence on which Breuer based in 1891 the suggestion that shear force is the adequate stimulus for vestibular receptors. More recently, Trincker's (1959) experiments lent direct support to this idea for they showed that tangential displacements of the statolith membranes elicited electrical potential changes in macular cells, whereby the direction of potential change depended on the direction of the mechanical displacement. This latter finding appears to attribute functional significance to the asymmetrical placement of the kinocilium in the sensory hair bundle which was first described by Flock (1964) and Spoendlin (1964) for the utricular maculae. Moreover, the abundant experimental evidence of recent years indicates that morphological polarization is a common design principle of hair cell receptors, and accounts for their directional selectivity (Flock, 1971).

If directional selectivity to bending by shear force determines indeed the adequate stimulus for each receptor in the otolith organ, it becomes pertinent to ask whether the activity in first order statoreceptor afferent nerve fibres preserves the response characteristics of the receptors. The alternative possibility would be that either the nature of the stimulus transduction at each receptor or the convergence of different receptors to individual afferent nerve fibres introduces some change in the stimulus representation.

In a qualitative manner, existing neurophysiological, behavioural and psychophysical data appear to indicate that at least some of the features of the presumed receptor response do remain preserved. Lowenstein & Roberts (1950) found that discharge frequency in afferents from the otolith organs of the thornback ray varied as a sine function of the angular head position as is expected if shear force is the effective stimulus. At a more complex level of experimental analysis, Von Holst (1950) identified shear force as the adequate stimulus for the statolith organ of fishes on the basis of their behaviour in centrifugal force fields. Furthermore, studies in man implicate shear force on vestibular statoreceptors as the stimulus for the ocular countertorsion reflex (Miller, 1961), and provide suggestive though indirect evidence that receptors with different directions of preferred sensitivity can affect different eye muscles (Fluur, 1970).

If these latter inferences are correct, one would be led to believe that information on head position reaches the central nervous system in a form which is similar to that generated by the otolith receptors. Our experiments were designed to examine the validity of this proposition. For this purpose, we recorded the activity of single eighth nerve axons during tilt of the

head relative to a reference plane. In addition, we designed a computer simulation model which calculated the shear force which would act on receptors with a given direction of preferred sensitivity. The question we wished to answer was whether over a series of head positions, computed shear force acting on receptors and discharge rate in statoreceptor afferents followed the same quantitative relation, or not.

By this approach a class of first order vestibular afferents was identified whose discharge frequency varied with head position as did the magnitude of shear force computed for individual receptors, each with a preferred direction of sensitivity. The majority of the spatial orientations of maximal sensitivity displayed as unit vectors defined a surface which is inclined by approximately 30° with reference to the horizontal plane of the Horsley–Clarke co-ordinate system. Accordingly most statoreceptor afferents are maximally sensitive to position changes when the cat's head is at or near its normal position.

METHODS

Subjects and preparations

The experimental animals were adult cats, anaesthetized I.P. with sodium pentobarbitone (35 mg/kg). Following venous catheterization and tracheal intubation, anaesthesia was maintained by supplementary doses of sodium pentobarbitone.

After the head was mounted in a stereotaxic instrument, the right vestibulocochlear nerve was exposed at its exit from the internal auditory meatus by opening the bony cover of the cerebellar fossa, and rapidly aspirating the flocculus and adjacent portions of the right cerebellar hemisphere. To improve the access to the nerve for micro-electrode impalement, the top of the internal auditory canal was removed with dental burrs for 1–2 mm lateral to the internal auditory meatus (Gacek, 1969).

While the head was still in the stereotaxic device, a chamber was sealed to the skull. This chamber was then rigidly suspended on a supporting framework in a manner which insured consistency of stimulus definition from preparation to preparation. This standardized procedure for head positioning consisted of placing the animal's Horsley–Clarke horizontal plane zero, 10 mm above and parallel to the turntable's horizontal plane (see Pl. 1). Furthermore, the midpoint of the interaural axis (i.e. the point 0,0,–10 in the Horsley–Clarke co-ordinate system) coincided with the centre of the turntable. The earbars were then removed and the animal's body was firmly supported so that the position of the body relative to the head remained unaltered during movements of the turntable. Throughout the experiment, rectal temperature was maintained at 35–38° C with heating pads.

The turntable which was used enabled rotation around the naso-occipital and interaural axes at constant velocities from 0·1 to 25°/sec (Werner & Whitsel, 1968). Angles of rotation could be read from dials mounted on each axis, and corresponding voltages were transmitted to the computer for analogue to digital conversion (see *Recording procedures* section). Each axis was capable of maintaining any preset position with a maximum static error of less than one degree.

Recording procedures

All recordings were made using capillary micropipettes filled with 3N-NaCl. Electrode impedance was measured with square wave pulses (1000/sec), and ranged

from 15 to 30 MΩ. The micro-electrode was inserted through the top of the chamber which together with the rest of the chamber and the skull formed a fluid-filled system, minimizing brain pulsations and insuring stability of single unit recording in spite of the position changes of the whole body during turntable motions. The electrode was positioned visually near the surface of the nerve which was then covered with a 3·0 % agar suspension in 0·9 % NaCl at 37° C to further improve stability (Goldberg & Fernandez, 1971).

The potential difference between the micro-electrode and an indifferent electrode inserted into the left temporal muscle was amplified by a cathode follower (Sanlab 610A), further amplified and filtered (Tektronix 3A9 preamplifier, at 100 c/s to 20 Kc/s filter settings), and led to an audio monitor, and a differential amplitude discriminator (DAD). Time intervals between successive discharges were measured on line with a LINC-8 computer with a resolution of 250 μsec. In addition, the calibrated analogue voltage across potentiometers mechanically coupled to the turntable axes provided the input to an analogue to digital converter (10 bits precision), whose value was read and recorded by the computer each time it read its internal clock (i.e. each time a spike occurred). Collection of data usually proceeded until the memory of the computer was filled (1020 spikes), at which time the stored data were written on to magnetic tape for later analysis.

RESULTS

General response properties

In thirty-seven cats, a total of 327 single units were isolated which responded to changes in head position with a change in discharge frequency. This sample does not include afferents specifically responsive to acceleration (see Goldberg & Fernandez, 1971; Tomko, 1971). Of these, 283 units (86 % of the sample) displayed the highly regular and periodic discharge sequences which earlier investigators have found to characterize statoreceptors under various experimental conditions (Lowenstein & Roberts, 1950; Rupert, Moushegian & Galambos, 1962; Vidal, Jeannerod, Lifschitz, Levitan, Rosenberg & Segundo, 1971). A discharge train was classified as regular if its coefficient of variation was less than 5 %. The forty-four remaining units (14 %) were irregularly discharging.

One of the most conspicuous characteristics of the regularly discharging units was the high degree of replicability of their discharge rates upon return to the same position. Another characteristic feature was the promptness with which a new discharge rate was reached upon movement to a new position. This is documented in Text-fig. 1, which displays the response of a regularly discharging unit prior to, during, and after a 30° rotation. The rapid attainment of a steady discharge rate at a new position implies that instantaneous discharge rates during rotation reflect closely the steady discharge rate which would obtain if the head had been held stationary at each angular position along the rotation.

Statoreceptor responses at fixed positions. The discharge rate was measured with the head resting in various pitch and roll positions. In Text-fig. 2, an

example of data obtained in such a manner is plotted as large solid points; the distance of these points from the origin represents in this display the mean discharge rate over 1020 spikes for each of the fixed angular positions. One rotational axis was always held constant, either at 0 or $-90°$; the different positions were 30° apart, measured with respect to the other axis.

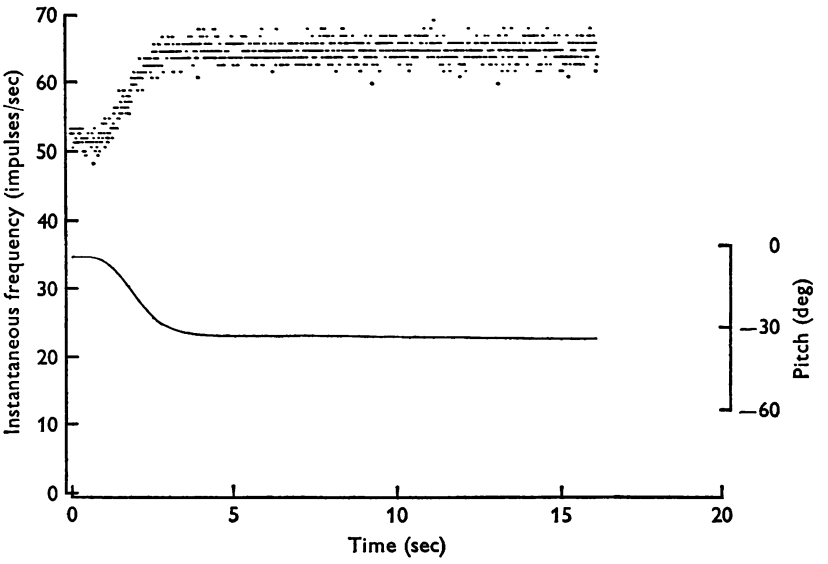

Text-fig. 1. Instantaneous discharge frequencies, displayed as fine points, of a regularly discharging statoreceptor afferent fibre before, during, and after a 30° rotation around the pitch axis, with roll held constant at 0°. The continuous line represents the pitch position measured by the potentiometer of the turntable axis concomitantly with the acquisition of neural data (see Methods). Pitch position is calibrated by the ordinate at the right.

Parts *A* and *B* show that discharge frequency increased when roll was held constant at either 0 or $-90°$, and the head rotated in the nose upward direction on pitch. Rotation around the roll axis in the left upward direction with pitch held constant at 0° (part *C*) likewise resulted in an increase in discharge frequency.

Statoreceptor responses during slow motion. Since one objective of our study was to examine rigorously the validity of a statoreceptor model (see next section), it was required that data be obtained for closely spaced angular positions around as many complete 360° perimeters as possible. To obtain these measurements of discharge rates at fixed positions would be the ideal procedure. However, the duration of time during which a single unit could be held in isolation for recording at many different head positions was the limiting factor since isolation rarely extended beyond 30–45 min.

Consequently, an alternative data acquisition procedure was applied. Its validity depended on examining whether the stationary discharge rate at each of a series of fixed positions could be replicated by the instantaneous discharge rate at each of these same positions, when the preparation traversed them at a slow velocity. Apart from the expediency of such data

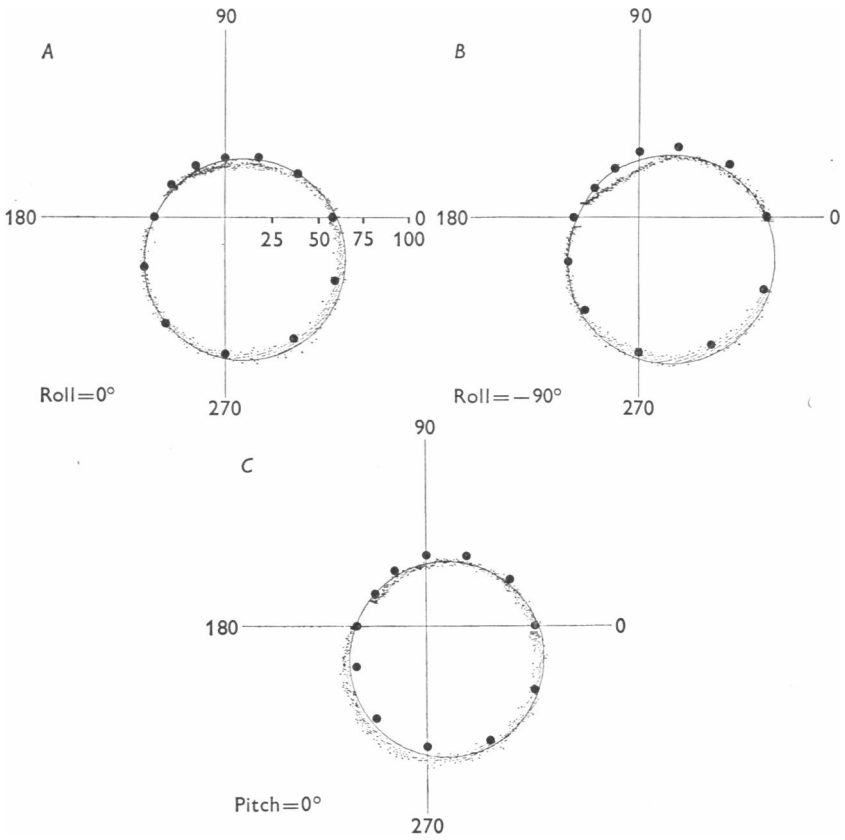

Text-fig. 2. A comparison of discharge rates collected at a series of fixed positions (large solid points) with instantaneous discharge rates (fine points) during a slow rotation (10°/sec) displayed in a polar co-ordinate system. In these co-ordinates, the distance of each point from the origin represents the discharge frequency. The discharge frequency scale indicated in *A* is the same for all three plots. Nose-downward pitch angles are plotted as positive angles, as are left ear-downward roll angles.

In *A*, the roll axis was held constant at 0° and a pitch rotation performed; in *B*, roll was equal to −90° with a 360° rotation of pitch. For each of the stimulus conditions, *A* and *B*, the computed relationship between head positions and discharge frequency is superimposed as a continuous curve passing through the data points. In *C*, the position of the pitch axis was held constant and roll varied.

collection, the substitution for stationary data of those obtained during slow rotation through 360° would offer the advantage of characterizing the entirety of the position-response relationship as an essentially continuous curve, rather than by a sequence of isolated sample points.

A comparison between discharge rates collected at a series of fixed positions (large solid points in Text-fig. 2) with instantaneous discharge rates obtained during slow rotation traversing these same positions is illustrated in the same Figure. The data obtained from this unit in the course of rotating the turntable at a velocity of 10°/sec around the corresponding axes are superimposed as fine dots; the distance of each point from the origin represents the reciprocal of time intervals between two successive discharges (i.e. instantaneous discharge frequency). It is apparent that the maximum and minimum discharge frequencies and the angular positions of their occurrence closely correspond under both conditions of data acquisition.

The slight differences in frequency evident in Text-fig. 2 between data collected at fixed positions and data collected with the animal in motion are an expression of the relatively small role which dynamic characteristics play in affecting the activity of regularly discharging statoreceptor afferents, at least at low velocities of rotation. Differences in discharge rates between a static position and a rotation through that same static position at velocities up to 25°/sec never exceeded 5 % in our control experiments. This difference is also comparable to that observed by Vidal *et al.* (1971). Moreover, the dynamic contribution appears to have primarily 'local' effects on some parts of the stimulus-response relationship, and does not affect the positions at which the maximum and minimum discharge frequencies occur. The comparison of data collected in a fixed position with those obtained during movement is based on entirely different sample sizes, the former consisting of 1020 discharges for each of the angular positions studied, and the latter consisting of 1020 discharges for a range of 360°.

Position-response relationships. The shear force hypothesis of Breuer (1891) implies that the force acting on vestibular statoreceptors is a sinusoidal function of head position. Measurements of discharge rate in vestibular afferent nerve fibres of elasmobranchs suggest that this relationship between force acting on receptors and head position remains preserved in the stimulus transduction from receptors to afferents (Lowenstein & Roberts, 1950; Schoen, 1957). Our data follow the same general pattern and, in addition, permit the appreciation of the role of directional selectivity of the afferents, much as is expected on morphological grounds for the receptors (see Lindeman, 1969). This point is illustrated in Text-fig. 3 which depicts the relation between discharge frequency (f) and pitch position (P) when 360° pitch rotations are performed with the head in

different roll positions. It is apparent that all three curves in this figure have the appearance of sine functions, differing, however, in their phase relations and peak frequency. This could not occur if the afferent responded equally to shearing force acting in any direction.

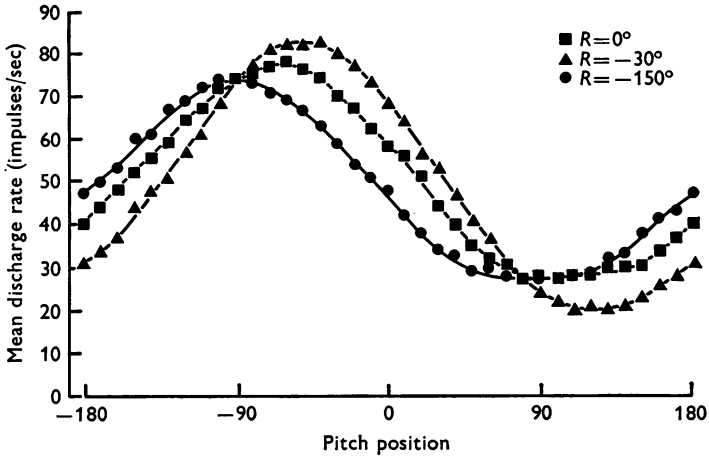

Text-fig. 3. Discharge rate plotted as a function of pitch position for three different roll positions (R = 0°, −30°, and −130°). Each discharge rate was obtained from the number of impulses in a 100 msec period. During data collection, the turntable rotated at a velocity of 10° per sec. The 100 msec periods for neural data collection never encompassed more than a 2° change of turntable position in the course of its rotation.

For uniformity of further analysis, we defined the phase shift as that shift along the pitch position axis which aligned the points of maximal discharge rate with a pitch angle of +90°. In this normalized form, the sinusoidal response functions can be subjected to a linear regression analysis if the independent variable is plotted as the sine of the head position corrected for phase angle.

The general result of these analyses was that the residual variance around the linear regression and more importantly, any systematic departure from the regression line, was reduced when the dependent and independent variables were transformed to logarithmic scales (see Text-fig. 4). Therefore, we concluded that the relation between the sine of angular position θ corrected for phase angle θ_0, and discharge rate (f) in stato-receptor afferents is best described by a power function of the general form:

$$f - f_0 = K\,(\sin(\theta - \theta_0) + 1{\cdot}0)^n, \qquad (1)$$

where K is a constant of proportionality and n reflects the curvature of the power function.

To obtain the numerical value of the exponent, n, the following procedure was followed: as a point of departure, the value of the minimal-discharge rate observed for the positions under study was taken to be f_0, which fulfils in eqn. (1) the role of spontaneous activity, that is, activity present in the absence of any effective shear force on the receptor. For different units, this value ranged from 0 to 30 impulses/sec. Since there was no guarantee that the positions sampled in the examination period of the unit also included a position at which the unit reached its minimum discharge rate, an iterative computational procedure was used to find that value of f_0 which would optimize the linear regression on eqn. (1). The

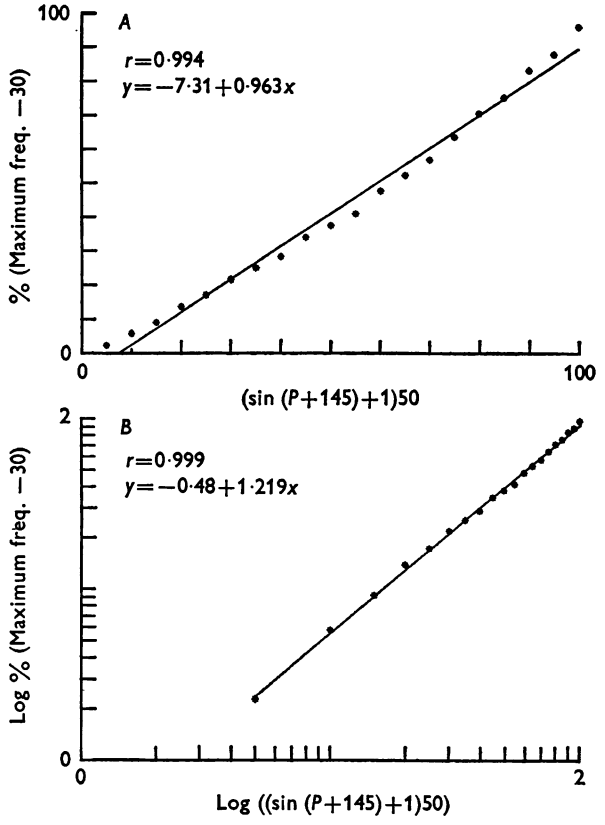

Text-fig. 4. Discharge rates (expressed as % maximum discharge rate) are plotted as a function of the sine of angular head position in linear (*A*) and logarithmic (*B*) co-ordinates ($\log_{10}$) for unit 28–13 where pitch was held constant and roll varied over 360°. The subtractive constant on the ordinate represents the value of f_0 (see eqn. (1)) while the additive constant on the abscissa represents the phase shift correction (see text for further explanation). Pearson correlation coefficients for the regression of the points on the plotted straight line are given as well as the equation for the fitted lines.

difference between experimentally determined and computed values of f_0 did not in any case exceed 5 impulses/sec.

The values of n (reflecting the slope of the regression line in the double logarithmic co-ordinate system) varied in this sample from 0·9 to 1·6 with a modal value of 1·3; correlation coefficients ranged between 0·947 and 0·999.

Mathematical modelling of statoreceptor responses

Definitions and assumptions. For the purpose of evaluating the implications of shear force hypothesis and receptor polarization in quantitative terms, several definitions and assumptions needed to be specified. First of all, a shear force acting on the receptors depends on the mass of the otolithic membrane, the viscosity of the suspending material, and the restoring forces which counteract shearing movements, as well as the buoyant effects of the endolymph (Trincker, 1962). In the present study, we have assumed that gravity is the most significant force acting on otoliths, and further, that their time constant is sufficiently small to permit neglecting the effects of damping.

In the second place, the anatomical findings alluded to in the introduction (e.g. Flock, 1964; Lindeman, 1969) suggest that there is for each receptor a particular spatial direction in which shearing is most effective. This direction will be termed the receptor polarization vector.

Computations of relative shear force. Following the convention adopted by Werner, Sacks & Firest (1969), the Euler co-ordinate System was chosen. The important point is that two axis systems need to be considered: one axis system (x, y, z) is measured with respect to the gravity field, which is stable in absolute space; the other (x', y', z') is defined by our standardized procedure for head positioning in the turntable, and is floating with respect to absolute space in the gravity field. In this latter system, the x' axis is the interaural line; the y' axis is the naso-occipital line, and the z' axis lies perpendicular to the $x'-y'$ plane. The intersection of these axes is the point $0,0,-10$ in the Horsley–Clarke co-ordinate system.

The first requirement for the computation of shear force is to formulate an expression which determines that component of the gravity vector G, which is colinear with the receptor's polarization vector. In the starting position of the turntable, when the head axes (x', y') and turntable axes (x, y), both lie in the horizontal plane of absolute space, this component of gravity is defined by the matrix product

$$G_e = \begin{vmatrix} 1 & 0 & 0 \\ 0 & \cos p & \sin p \\ 0 & -\sin p & \cos p \end{vmatrix} . \begin{vmatrix} \cos r & 0 & -\sin r \\ 0 & 1 & 0 \\ \sin r & 0 & \cos r \end{vmatrix} . \begin{vmatrix} 0 \\ 0 \\ -1 \end{vmatrix}, \qquad (2)$$

where p and r are the spherical co-ordinates of the polarization vector in the axis system of the head, and the matrix $\begin{vmatrix} 0 \\ 0 \\ -1 \end{vmatrix}$ represents the force of 1 g acting in a downward ($-z$) direction (for computational details, see Hollingsworth, 1967).

Next we develop the computation for the effective component of the gravitational force when a rotation of the turntable around the pitch axis by P degrees and around the roll axis by R degrees is performed. The task is to determine the relation between the angles P and R (measured on pitch and roll axis dials, respectively, of the turntable) and the component of gravitational force acting on the receptor in its new position in the gravity field. This requires two transformations. In the first place, the head axis system itself undergoes a change of position with respect to the gravity field. The following pair of matrices defines a new co-ordinate system of head position in terms of the dial readings P and R:

$$x\,(P) = \begin{vmatrix} 1 & 0 & 0 \\ 0 & \cos P & \sin P \\ 0 & -\sin P & \cos P \end{vmatrix}, \tag{3}$$

$$y\,(R) = \begin{vmatrix} \cos R & 0 & -\sin R \\ 0 & 1 & 0 \\ \sin R & 0 & \cos R \end{vmatrix}. \tag{4}$$

An important point is that the rotations around the pitch and roll axes must be performed in a fixed order: for, any rotation of one axis places the second axis into a new spatial position, redefining its orientation in the gravity field. Therefore, the effect of a rotation around this second axis is dependent on the preceding rotation around the first axis. This non-commutativity of rotations is also reflected in the matrix eqns. (3) and (4). In the conduct of the experiments as well as in the computer simulation model we adopted the convention to have pitch rotations of the turntable precede roll rotation.

Secondly, the spherical co-ordinate system of the polarization vector, originally defined with reference to head and turntable axis system lying in the horizontal plane of absolute space (see above), needs to be referenced to the new co-ordinate system of head position. This is accomplished by eqns. (5) and (6)

$$x'\,(p) = \begin{vmatrix} 1 & 0 & 0 \\ 0 & \cos p & \sin p \\ 0 & -\sin p & \cos p \end{vmatrix}, \tag{5}$$

$$y'(r) = \begin{vmatrix} \cos r & 0 & -\sin r \\ 0 & 1 & 0 \\ \sin r & 0 & \cos r \end{vmatrix}. \quad (6)$$

The combined application of transformations ((3), (4) and (5), (6)) to the gravity matrix makes it now possible, for any pair of dial readings P and R on the turntable, to compute the component of gravity acting on a receptor whose polarization vector in the normalized head position (referenced to the horizontal plane) was given by the spherical co-ordinates p and r.

Thus one obtains by matrix multiplication of expressions (3) to (6) with the gravity matrix:

$$\left.\begin{aligned} G_e &= y'(r)\, x'(p)\, y(R)\, x(P)\, G \\ G_e &= \cos P \sin R \cos r - \sin P \sin p \sin r + \cos P \cos R \cos p \sin r \end{aligned}\right\} \quad (7)$$

where the value of G_e can range from -1 to $+1\,g$. The values of G_e represent relative shear forces for they do not take into account the actual mass of the otoliths, which is assumed constant.

Stimulus sequences most often consisted of rotations around the pitch axis with $R = 0°$ or $-90°$. For each of these sequences, a simplified expression for G_e can be derived from eqn. (7).

When $R = 0°$ and P is variable,

$$G_e = (\cos P \cos p \sin r - \sin P \sin p \sin r), \quad (8)$$

where $R = -90°$ and P is variable,

$$G_e = (-\cos P \cos r - \sin P \sin p \sin r). \quad (9)$$

Eqns. 8 and 9 can be used to predict the shear force acting on a receptor with a given sensitivity vector (i.e. p and r) in any combination of positions P and R. Alternatively, these same relations can be used to estimate the value of the sensitivity vector orientation (p and r) if the changes in shear force with variations in angle P are known.

Comparison between experimental data and model predictions

As stated in the introduction, our principal objective was to subject the predictions from shear force hypothesis and receptor polarization to a quantitative comparison with the neural activity in statoreceptor afferents. The experimental data described in the previous section have lent support to the idea that both notions are applicable to the interpretation of the neural activity in these afferents. In particular, the observed phase shifts

in the stimulus-response relationships were in a first approximation found to be attributable to a directional selectivity of first-order afferents not unlike that determined by the morphological polarization of the receptors themselves. Moreover, these data indicated a slight degree of non-linearity between position and response, best represented by a power function.

In this section, we plan to refine the interpretation of the data by comparing them with quantitative predictions from the computational model. Specifically, the line of thought is as follows: if the first-order afferents from the statoreceptors are as specific for a preferred direction of shear force as the receptors are presumed to be in the model, eqns. (8) and (9) should describe the relation between discharge rate and head position, except for a power function transformation (see eqn. (1)). Conversely, starting with discharge rates at different head positions, it should be possible to estimate for each afferent a sensitivity vector orientation (in terms of its vector components p and r), much as the same equations would predict this vector if shear force itself were accessible to direct measurement. Next, it needs to be shown that estimates of p and r, obtained from some of the neural data of an afferent would permit the model algorithm to generate additional neural response functions to variations of head position which were experimentally obtained for the same afferent, but not used for the estimation of p and r. If the model indeed permitted one for each afferent, to generate the entire set of recorded data from a limited subset of these data, it would follow that statoreceptor afferents preserve the directional selectivity to excitation by shear force which is presumed to be operative at the level of the receptors.

Each unit included in this comparison belonged to the class of regularly discharging neurones as defined earlier, showed negligible response transients due to motion, and met the criterion of replicability of response. The most severe restriction in the size of the unit sample available for the comparison resulted from the frequent impossibility of collecting adequate amounts of data for the various head positions required for the calculation of p and r (i.e. polarization vector orientation) using equations (8) and (9). This circumstance was by far the most demanding requirement, and further reduced the number of 283 regularly discharging units isolated, to the ninety-five neurones which form the basis for the subsequent analysis.

Procedure for estimating the orientation of a polarization vector (p and r) from neural data. In this section, we examine whether discharge rate in afferents can be described by the computer model of shear force acting on receptors. For this, we apply a power transformation (see eqn. (1)) to computed shear force to obtain predicted discharge frequencies and compare the result with observed discharge rates. Eqns. (8) and (9) can then be used to obtain solutions for p and r, respectively. The first step consists

of estimating from data such as those displayed in Text-fig. 2 at which angle of pitch (P) discharge frequency is maximal when the roll angle (R) is 0°; and at which angle of pitch (P) discharge frequency is maximal when the roll angle (R) is held at $-90°$. The first value will be designated P_1 and the second, P_2. These values are read off from data displays such as illustrated in Text-fig. 2. The maximum discharge frequency was found to be a feature which could most reliably and reproducibly be estimated in this manner.

When the above criteria are adhered to, eqn. (8) yields the following solution:

$$p = -P_1 \tag{10}$$

and eqn. (9) reduces to:

$$r = \arctan\left(\frac{\tan P_2}{\sin p}\right). \tag{11}$$

Application of these formulae ((10) and (11)) to the data plotted in Text-fig. 2A and B yields values of p and r of 65° and 125° respectively, for this unit.

The values of p and r thus determined from data collected with two rotations at different combinations of roll and pitch enabled the simulation model to compute shear forces presumed to be effective at each position of the two rotations chosen for the computation of p and r, and any other position as well. The test of the validity of the model assumptions, which included the procedure leading to the determination of p and r in the first place, consists of the degree to which discharge rates at positions other than those used for the computation of p and r can be matched. To permit this comparison between experimentally determined and computationally predicted discharge rates, the non-linear relationship between shear force and discharge rate which the data of Text-fig. 4 suggest to be of the form of a power function (eqn. (1)) must be taken into account.

Procedures for comparing data with model predictions. To enable comparison between model computations of shear force and experimental data, two transformations were required. In the first place, the stimulus scale (G_e) was linearly transformed according to eqn. (12), to ensure that negative numbers would not occur.

$$G'_e = 0{\cdot}5\ (G_e + 1) \tag{12}$$

Secondly, the non-linearity of stimulus transduction was accounted for by eqn. (13):

$$\log\ (f - f_0) = \log K + n \log G'_e. \tag{13}$$

Using the values of n determined by eqn. (1), these discharge rates were generated by a digital computer programme which evaluated eqn. (13)

repeatedly for small stepwise increments of the angles P and R. This enabled prediction of discharge frequency for any rotation around the pitch or roll axis or any combination thereof. These frequencies were displayed in a polar co-ordinate system making it possible to compare readily the computed curve with the experimental data by visual inspection. An example is shown in Text-fig. 2 in which the continuous closed curve passing through the data points represents the computed response function for each of the three rotations shown.

Note that for the estimation of p and r for this unit, only the experimental data of parts A and B are used. Hence the replication of these experimental data by the model is circuitous in the sense that the model merely generates the data from which it received the numerical estimates of a polarization vector. However, the data of part C, which did not supply measurements to the model, are also replicated by the model. The point is that some small subset of the experimental data can provide the numerical estimates which enable the model algorithm to predict responses at other head positions as well.

The systematic application of this process is illustrated for three different units in the left-hand column of Text-fig. 5. In each row labelled A to C, an entire family of experimentally determined position-response functions is displayed in a three-dimensional co-ordinate system viewed in perspective. Of each of these families, only two position-response functions were used to obtain the estimates for p and r of the resultant polarization vector of the respective afferent. These estimates permitted the simulation model to generate for each unit entire response surfaces, shown in the right-hand column of Text-fig. 5, which correspond in each instance with striking detail to the available experimental data.

A similar correspondence between experimental and computed response functions was established for all ninety-five units. Therefore, we conclude that the close agreement between obtained and predicted discharge properties for such a large variety of different positions adds considerable credence to the validity of the computational procedures and the assumptions underlying them.

DISCUSSION

The correspondence between discharge frequencies in statoreceptor afferents and gravitational force acting on directionally polarized receptors, together with a power function transformation to account for stimulus transduction, answers the principal question we attempted to resolve: namely, whether statoreceptor afferents possess directional sensitivity of a degree similar to that presumed on morphological grounds to be operative for receptors. The evidence which we presented supports the notion that

each statoreceptor afferent behaves as if its activity were determined by a uniquely defined polarization vector. This could occur either because all receptors supplied by one afferent have the same polarization vector; or else a resultant polarization vector may be formed by convergence from different receptors. In the guinea-pig at least, there is the suggestion that the ratio of statoreceptors to first-order fibres is much greater than one to one (Gacek & Rasmussen, 1961; Lindeman, 1969) implying that convergence does occur at this level.

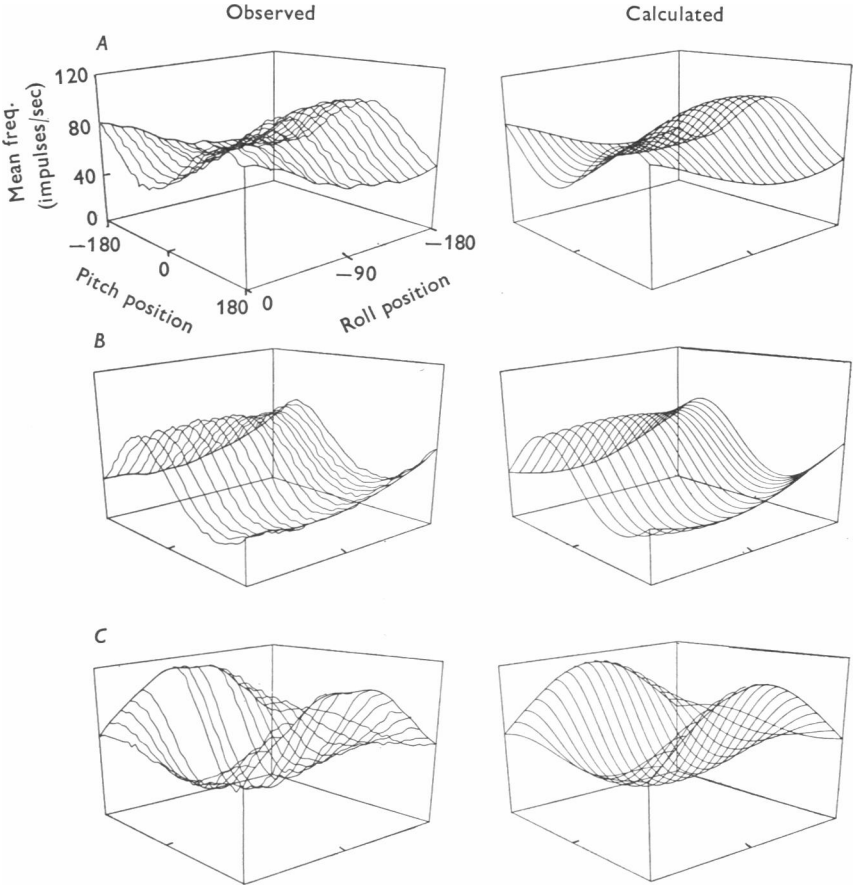

Text-fig. 5. Comparison of the experimentally determined discharge frequencies of three first-order afferent vestibular nerve axons (left column) with predicted frequencies (right column) calculated from eqns. (7), (12), and (13) (see text). Discharge frequency is represented in each case as a surface whose domain encompasses all possible head positions. In each graph, the pitch and roll angles of head position are plotted on the two abscissae, and discharge frequency is plotted on the ordinate. Ordinate scales are the same in all cases, as are the respective abscissa scales.

The display of Text-fig. 5 requires some further comment. As stated before, this displays characteristic discharge rates in vestibular stato-receptor afferents for many different combinations of roll and pitch positions in the form of surfaces in perspective space. Although informative with respect to the comparison between experimental data and model predictions, this form of display tends to detract from their physical meaning, for in reality, each of these surfaces is a closed sphere-like three-dimensional shape. This is evident from inspection of the perspective co-ordinate system used (see Text-fig. 5) for the pitch co-ordinates $\pm 180°$ (with roll $= 0°$) coincide in space with the $0°$ co-ordinate of the same axis when roll $= -180°$. Hence, this co-ordinate system contains the instruction, as it were, to bend the display such that these three co-ordinates come to superimpose. The resultants of such an operation are sphere-like shapes, of which one is depicted in Pl. 2. This shape tells the story of the polarization vector in a form which will appeal more directly to intuition than do the displays of Text-fig. 5.

Thus, there is a simple 'locus' of head positions (shown in Pl. 2 as a bulging of the surface of the sphere), which results in maximal excitation of each afferent. In the data of Pl. 2, this locus of points may be described by a vector pointing towards the left ear; that is to say, a rotation of the left ear downwards by 90° brings the afferent to its maximum discharge rate. This vector is the sensitivity vector orientation which has been described above. Its orientation determines the spatial head positions to which the afferent neuron is optimally 'tuned'.

Orientation of these resultant polarization vectors determined for the ninety-five units which provided the data for the comparisons with the simulation model are depicted in Pl. 3 as points on a sphere representing a cat's head. On the equator of the sphere vectors lying in the horizontal plane as defined in the method section are plotted. The position of the right ear and the nose are identified for orientation, as well as the top of the head (used to define z axis; see Methods). It should be kept in mind that each point in Pl. 3 represents the end-point of a unit vector which passes through the intersection of the head axis system and represents the position of the polarization vector in the head axis system.That is, the difference between each of these vectors and the z axis is the amount by which the head would have to be rotated to maximally excite the afferent. For clarity, another illustration will be given; three vectors are depicted as lying on the meridian defined by the sagittal plane. One is directed toward the occiput, and two towards the nose. If we consider the unit represented by the vector directed toward the occiput, a rotation of the head on the pitch axis of 85° in the nose upward direction would bring its discharge rate to a maximum, while roll positions with the pitch axis held horizontal

would have little effect on its discharge. If plotted in a manner analogous to that of the data in Pl. 2, the position-response sphere of this unit would have its 'bulge' pointing toward the occiput and 5° below the Horsley–Clarke horizontal plane.

On first inspection of Pl. 3, it is apparent that the polarization vectors represented by the dots on the surface of the sphere are not randomly distributed. Instead, most of the points group in a band around the perimeter of the sphere. The perimeter most closely representing this band defines a plane which is tilted around the pitch axis by about 30° (nose upward) and around the roll axis by about 10° (right side up).

This characteristic distribution of the polarization vectors has a suggestive implication for the functional organization of the peripheral statoreceptor mechansim. It is important to remember that each point on the surface of the sphere represents the end-point of a polarization vector and that an afferent is maximally active if its polarization vector is colinear with gravity force. Hence the departure of polarization vectors from the direction of gravity force signifies the angle the head would have to rotate such that this afferent becomes maximally active. Now, looking at the sphere, it is apparent that with few exceptions none of the polarization vectors depicted by the dots on the surface of the sphere is colinear with gravity when the head is in its normal position. Instead, most lie midway between their maximally and minimally excitatory positions.

The implication of this distribution is that, as a population, statoreceptor afferents signal deviations from the normal head position (that is, with the Horsley–Clarke horizontal plane inclined 30° nose downward) with greatest sensitivity; on the average, this sensitivity amounts to 5 spikes/sec per 10° for each fibre. This distribution of directions of preferred sensitivity can account for the observation of Graybiel & Patterson (1955) in man that the oculogravic illusion occurs with minimal head position changes when the subject is sitting with his head in the normal position, and requires larger head position changes when the subject is lying; however, it fails to account for the virtual absence of the oculogravic illusion in the upside down position.

In our sample of afferents from the right ear, sensitivity vectors pointing to the right occur approximately three times as often as do vectors pointing to the left; hence, the statoreceptor afferents of each ear as a population, signal preferentially ipsilateral head tilt.

Although fibre sampling by the micro-electrode was expected to be purely at random, we frequently observed that fibres isolated in the course of individual micro-electrode penetrations across the nerve had similar preferred directions of sensitivity. Nevertheless, it seems surprising that our sample yielded with few exceptions sensitivity vectors which seemed

to form one homogeneous population, namely that grouped around the thirty degree inclined plane referred to earlier. Therefore, it appears that at least the majority of afferents both from utriculus and sacculus operate in the normal head position at the point on the position-response curve where sensitivity to change is greatest, and in this respect form functionally one common population.

One may ask to what extent the efferent pathways to the otolith receptors (Gacek, Nomura & Balogh, 1965; Pratt, 1969; Spoendlin & Lichtensteiger, 1966) may be capable of modulating the sensitivity of this population of afferents. Our preparations were anaesthetized and, therefore, in a state in which efferent innervation of statoreceptors has been shown to be essentially inactive (Gleisner & Henriksson, 1963). The conditions under which efferent innervation may modulate the statoreceptor responses remains a subject for further investigations.

Note added in proof

Since submitting this manuscript for publication, Fernandez, Goldberg & Abend published the results of a similar study on the squirrel monkey (*J. Neurophysiol.* (1972) **35**, 978–997) which these authors kindly made available to us before publication, as we did ours to them. Although the conceptual approach to the analysis of neural data is in both studies derived from an earlier technical report (Werner *et al.* 1969) and although many of the aspects of the findings are in concordance, there are differences in some of the conclusions. Fernandez *et al.* assigned each afferent to one of two distinct classes, one presumed to originate from the utriculus, the other one from the sacculus. On the other hand, with the random sample of afferents of our study, we were led to infer that by far the majority of the polarization vectors assemble around *one* common plane, namely a plane which is horizontal in the gravity field when the cat's head is held in its normal position. Hence, we concluded that the statoreceptor afferents form on the whole one common functional group, imparting maximal sensitivity for head position changes near the cat's normal head position.

This difference may reflect an essential dissimilarity in the peripheral statoreceptor mechanisms of cat and squirrel monkey. Alternatively, this difference may be accounted for by the fact that Fernandez *et al.* did not base their computations on the entire set of neural data which we found necessary to enable unambiguous assignment of polarization vectors. The availability of neural data at too few head positions may also account for the conclusion of Fernandez *et al.* that the stimulus-response relationship for activity of first-order statoreceptor afferents is linear, while the consideration of a larger set of measurements in our study made the nonlinearity of this relation apparent.

The initial phases of this project were supported by a Research Grant from the U.S. Air Force (AFOSR-66-1005C). Later phases were supported, in part, by NIH Grant MN 11682 and NB 07712, and by a grant from the Scottish Rite Committee on Research in Schizophrenia.

P.L. was supported during part of this project by Neurobiology Training Grant MH 11114; D.T. was during part of the project a predoctoral trainee, supported by the same Training Grant.

Part of the work reported here was performed by D.T. in partial fulfilment of the requirements for a Doctorate Degree. A preliminary report of this work has already been given (*Proc. Int. Union Physiol. Sci.* **9**, 350).

We thank Mr Donald Ferrera for his excellent photographic work.

REFERENCES

BREUER, J. (1891). Ueber die Function der Otolithen Apparate. *Pflügers Arch. ges. Physiol.* **48**, 195–306.

FLOCK, Å. (1964). Structure of the macula utriculi with special reference to directional interplay of sensory responses as revealed by morphological polarization. *J. cell Biol.* **22**, 413–431.

FLOCK, Å. (1971). Sensory transduction in hair cells. In *Handbook of Sensory Physiology*, vol. 1, ed. LOEWENSTEIN, W. R., pp. 396–441. New York: Springer.

FLUUR, E. (1970). The interaction between the utricle and the saccule. *Acta oto-lar.* **69**, 17–24.

GACEK, R. R. (1969). The course and central termination of first order neurons supplying vestibular end organs in the cat. *Acta oto-lar.* suppl. **254**, 1–66.

GACEK, R. R. & RASMUSSEN, G. L. (1961). Fiber analysis of the stato-acoustic nerve of guinea pig, cat and monkey. *Anat. Rec.* **139**, 455–463.

GACEK, R., NOMURA, Y. & BALOGH, K. (1965). Acetylcholinesterase activity in the efferent fibers of the stato-acoustic nerve. *Acta oto-lar.* **59**, 541–553.

GLEISNER, L. & HENRIKSSON, N. G. (1963). Efferent and afferent activity pattern in the vestibular nerve of the frog. *Acta oto-lar.* suppl. **192**, 90–103.

GOLDBERG, J. M. & FERNANDEZ, C. (1971). Physiology of peripheral neurons innervating semicircular canals of the squirrel monkey. I. Resting discharge and response to constant angular accelerations. *J. Neurophysiol.* **34**, 635–660.

GRAYBIEL, A. & PATTERSON, J. (1955). Thresholds of stimulation of the otolith organs as indicated by the oculogravic illusion. *J. appl. Physiol.* **7**, 666–670.

HOLLINGSWORTH, C. (1967). *Vectors, Matrices and Group Theory for Scientists and Engineers.* New York: McGraw Hill Book Co.

LINDEMAN, H. (1969). Studies on the morphology of the sensory regions of the vestibular apparatus. *Ergebn. Anat. EntwGesch.* **42**, 1–113.

LOWENSTEIN, O. & ROBERTS, T. D. M. (1950). The equilibrium function of the otolith organs of the thornback ray (*Raja clavata*). *J. Physiol.* **110**, 392–415.

MILLER, N. (1961). Counterrolling of the human eyes produced by head tilt with respect to gravity. *Acta oto-lar.* **54**, 479–501.

PRATT, L. (1969). A histochemical study of the course and distribution of the efferent vestibular fibers to the maculae of the saccule and utricule. *Laryngoscope, St Louis* **79**, 1515–1545.

RETZIUS, M. (1881). *Das Gehörorgan der Wirbelthiere.* Stockholm: Samson and Wallin.

RUPERT, A., MOUSHEGIAN, G. & GALAMBOS, R. (1962). Micro-electrode studies of primary vestibular neurons in cat. *Expl Neurol.* **5**, 100–109.

SCHOEN, L. (1957). Mikroableitungen einzelner zentraler Vestibularis-neurone von Knochenfischen bei Statolithenreizen *Z. vergl. Physiol.* **39**, 399–417.

SPOENDLIN, H. H. (1964). Organization of the sensory hairs in the gravity receptors in utricle and saccule of the squirrel monkey. *Z. Zellforsch. mikrosk. Anat.* **62**, 701–716.

SPOENDLIN, H. & LICHTENSTEIGER, W. (1966). The adrenergic innervation of the labyrinth. *Acta oto-lar.* **61**, 423–434.

TOMKO, D. (1971). Discreteness of organization of primary afferent neurons in the vestibular sytem of the cat. Unpublished Doctoral dissertation, University of Pittsburgh.

TRINCKER, D. (1959). Neuere Untersuchungen zur Elektrophysiologie des Vestibular-Apparates. *Natürwissenschaften* **46**, 344–350.

TRINCKER, D. (1962). The transformation of mechanical stimulus into nervous excitation by the labyrinthine receptors. *Symp. Soc. exp. Biol.* **16**, 289–317.

VIDAL, J., JEANNEROD, M., LIFSCHITZ, W., LEVITAN, H., ROSENBERG, J. & SEGUNDO, J. P. (1971). Static and dynamic properties of gravity-sensitive receptors in the cat vestibular system. *Kybernetik* **9**, 205–215.

VON HOLST, E. (1950). Die Arbeitweise des Statolithenaparates bei Fischen. *Z. vergl. Physiol.* **32**, 60–120.

WERNER, G. & WHITSEL, B. L. (1968). *The Activity of Afferent Nerve Fibers from the Vestibular Organ and of Neurons in the Vestibular Nuclei of Unanesthetized Primates.* Technical Report, No. 1 to U.S. Air Force Office of Scientific Research, Arlington, Va.

WERNER, G., SACKS, H. & FIERST, J. (1969). *Design and Evaluation of Experiments with Labyrinthine Statoreceptors.* Technical Report, No. 2 to U.S. Air Force Office of Scientific Research, Arlington, Va.

EXPLANATION OF PLATES

PLATE 1

The apparatus which was used to control the position of the animal with respect to the gravity field is illustrated. The rectangular frame (P) permitted rotation of the animal around the pitch axis. The circular frame (R) within it enabled rotation around the roll axis. Both rotations could be controlled by servo-motors (S). In this illustration, rotations of about 30° have been performed, the pitch rotation having brought the nose downward, and the roll rotation having brought the right ear upward.

The metal bar (B) which is visible at the centre of the circular frame was rigidly fixed with respect to the latter, and served to support both the head (H) and the micro-drive (M). The positions of the micro-electrode (E) and cathode follower (C) are also indicated.

PLATE 2

The discharge frequency of a hypothetical first order statoreceptor afferent neurone is plotted in three dimensions as a function of head position. The polarization vector of this unit is in the x' direction, or toward the left ear, and the x, y, z and x', y', z' co-ordinate systems coincide as they would with the head horizontal. Predicted discharge frequencies calculated from eqns. (7), (12), and (13) are plotted on an arbitrary, radius scale for all possible head positions. Insets A to C are two-dimensional polar co-ordinate plots which represent cross-sections of the main Figure in the y, z; x, y; and z, x planes respectively. The axis convention for inset Figures A to C is the same as in Text-fig. 4. These figures are redrawn from plots generated on the LINC-8 computer. The value of f_0 was 10, K was 90, and n was 1·3.

PLATE 3

The spatial orientations of the polarization vectors of the ninety-five statoreceptor afferent fibres from the right vestibular organ which were fully characterized in this study (see text). Four views of a sphere which, on its surface shows the head's co-ordinate system. In all four views, the heavy, horizontal line lies in the Horsley–Clarke horizontal plane. In A and B, the heavy vertical line perpendicular to the horizontal plane lies in the coronal plane, passing through the interaural axis; the intersection of the horizontal and vertical is the left ear in A, and in B is the right ear. The occiput is represented on the right in A and on the left in B. In C, the sphere in A has been rotated slightly, bringing into view a second heavy line perpendicular to the horizontal; this second line lies in the sagittal plane, and passes through the naso-occipital axis at its intersection with the horizontal at the occiput. Likewise in D, the sphere has been rotated to bring into view the intersection of the sagittal and horizontal planes at the occiput. In all views the finer lines are arranged 30° apart.

Each point on the surface of the sphere represents the spatial orientation of a statoreceptor afferent in the spherical co-ordinate system of the head (i.e. p and r, see text for details). The four views of the sphere show that these points cluster primarily on the right hemisphere (B and D), and that they cluster around a plane which is inclined about 30° (nose up) with respect to the Horsley–Clarke horizontal plane.

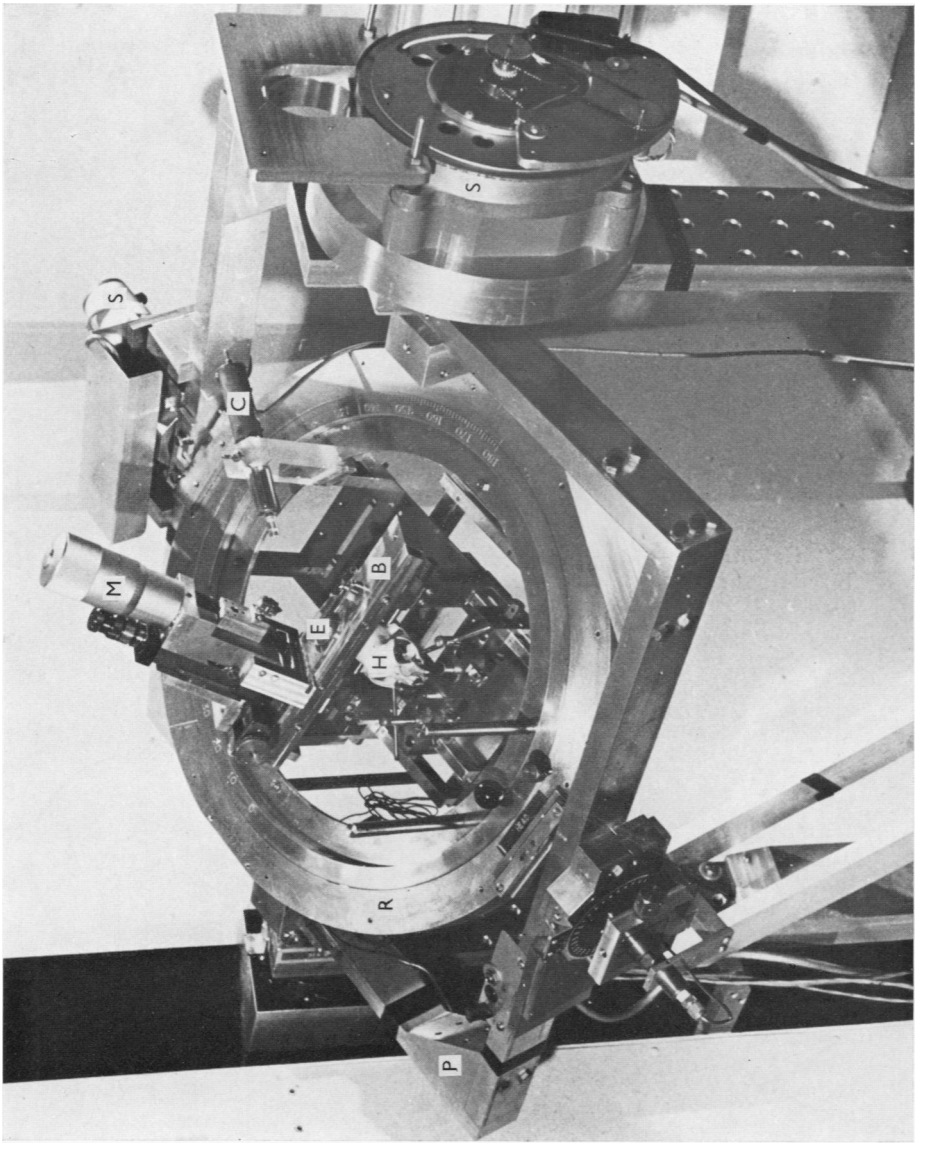
S
S
C
M
B
E
H
R
P

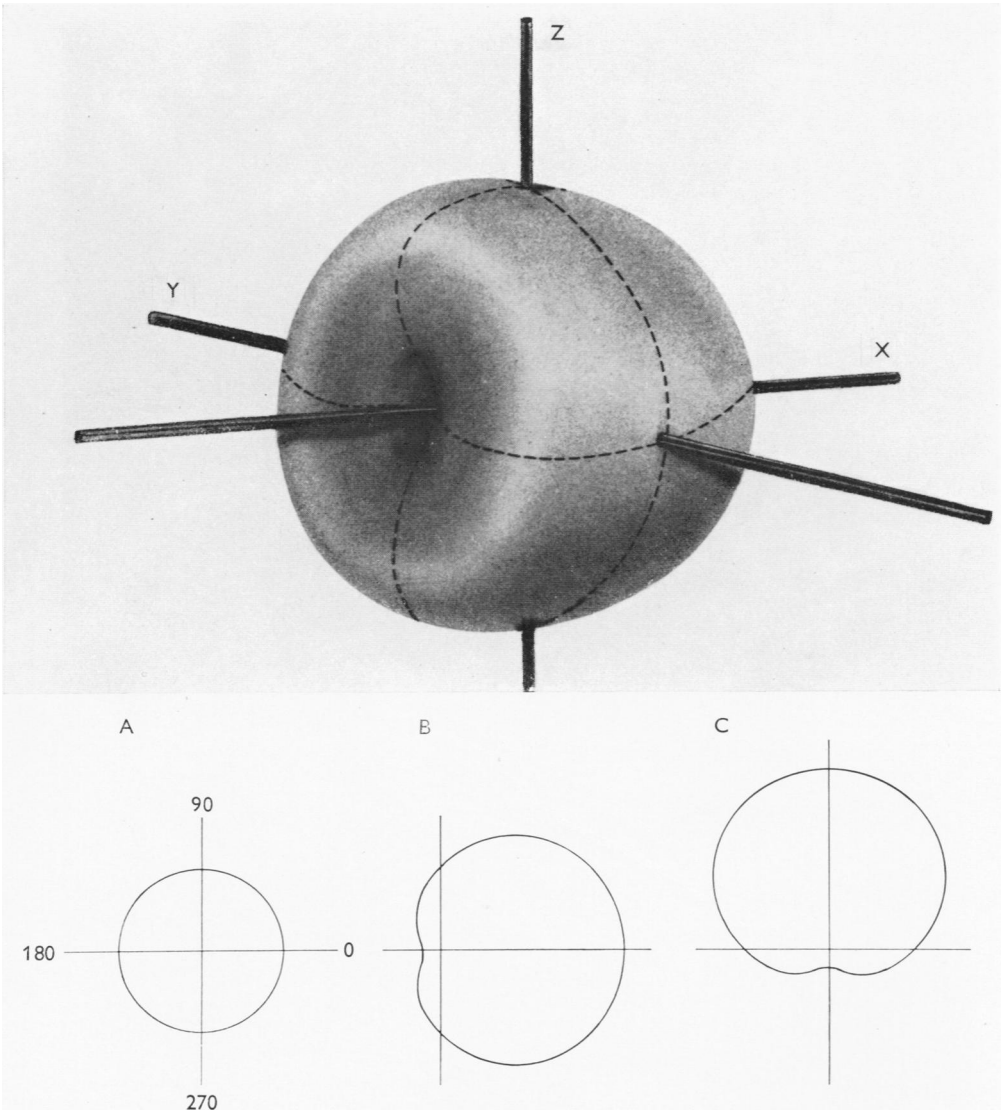
Z
Y
X
A
B
C
90
180
0
270

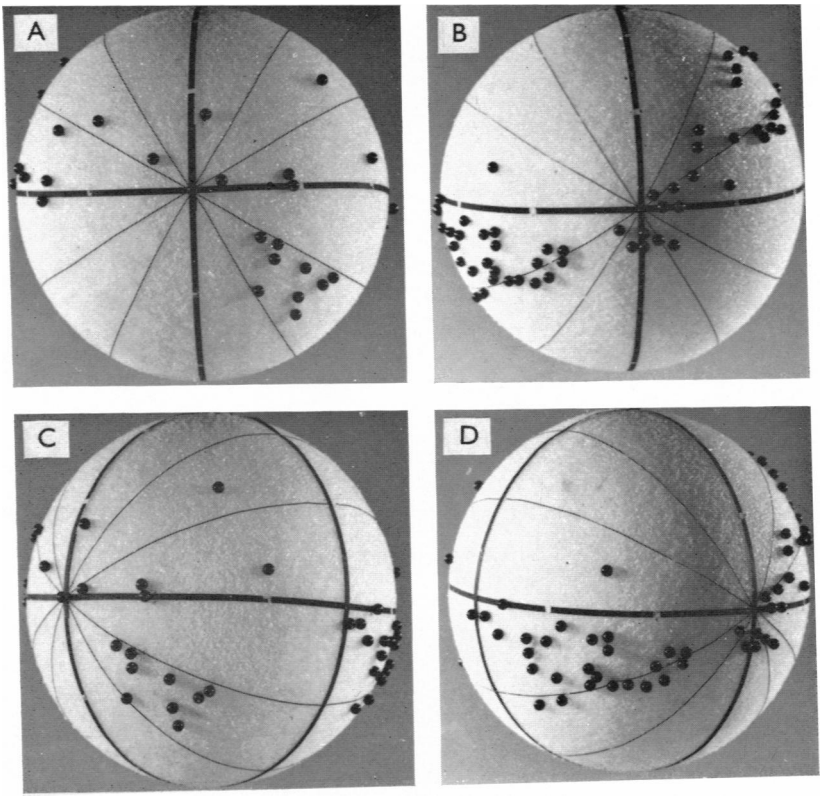
A
B
C
D